

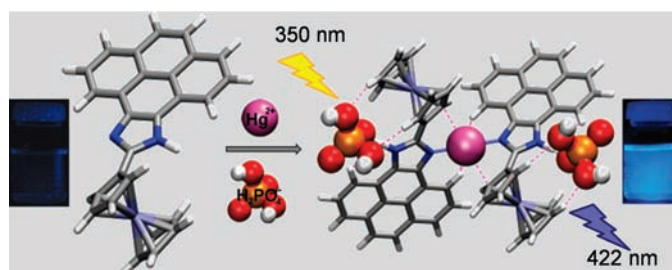
A Simple but Effective Dual Redox and Fluorescent Ion Pair Receptor Based on a Ferrocene–Imidazopyrene Dyad

María Alfonso, Arturo Espinosa, Alberto Tárraga,* and Pedro Molina*

Departamento de Química Orgánica, Facultad de Química, Universidad de Murcia, Campus de Espinardo, E-30100, Murcia, Spain

atarraga@um.es; pmolina@um.es

Received February 23, 2011



The ferrocene–imidazopyrene dyad, bearing the imidazole ring as the only receptor site, acts as a redox and optical molecular sensor for ion pairs, exhibiting an easily detectable signal change in the redox potential of the ferrocene/ferrocenium redox couple and in the emission spectrum. Perturbation of the emission spectrum follows the order $\text{Pb}^{2+} > \text{Hg}^{2+} > \text{Zn}^{2+}$ for cations and $\text{H}_2\text{PO}_4^- > \text{AcO}^-$ for anions.

The design of ion pair receptors that contain two quite different binding sites for the simultaneous complexation of cationic and anionic guest species is a new emerging and topical field of supramolecular chemistry. These multisite receptors are able to bind a single heteroditopic guest or simultaneously bind to nonidentical guests. The development of convergent ion pair hosts is a challenging problem in molecular design because the binding sites have to be incorporated into a suitably preorganized scaffold that holds them in close proximity, but not so close that species can interact.¹ However, despite their potential applications

in various fields, such as salt solubilization, extraction, and membrane transport,² the number of well-characterized ion pair receptors remains limited.³ In these systems crown ethers and π -electron donors, such as functionalized calixarenes, have been frequently utilized as cation binding units, while the anion is coordinated using Lewis acidic, electrostatic, or hydrogen bonding interactions.

(1) (a) Smith, B. D. In *Ion Pair Recognition by Ditung Receptors, Macrocyclic Chemistry: Current Trends and Future*; Gloe, K., Antonioli, B., Eds.; Kluwer: London, 2005; pp 137–152. (b) Kirkovits, G. J.; Shiriver, J. A.; Gale, P. A.; Sessler, J. L. *J. Inclusion Phenom. Macrocyclic Chem.* **2001**, *41*, 69–75. (c) Kim, S. K.; Sessler, J. L. *Chem. Soc. Rev.* **2010**, *39*, 3784–3809. (d) Gale, P. A. *Coord. Chem. Rev.* **2003**, *240*, 191–221.

(2) (a) Pelizzi, N.; Casnati, A.; Friggeri, A.; Ungaro, R. *J. Chem. Soc., Perkin Trans. 2* **1998**, 1307–1311. (b) White, D. J.; Laing, N.; Millar, H.; Parsons, S.; Coles, S.; Tasker, P. A. *Chem. Commun.* **1999**, 2077–2078. (c) Rudkevich, D. M.; Mercer-Chalmer, J. D.; Verboom, W.; Ungaro, R.; de Jong, F.; Reinhoudt, D. N. *J. Am. Chem. Soc.* **1995**, *117*, 6124–6125.

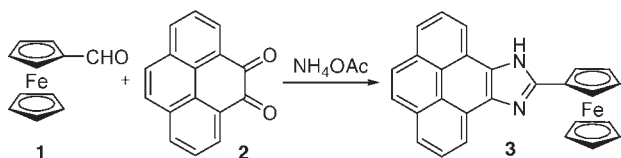
(3) (a) Reetz, M. T.; Niemeyer, C. M.; Harms, K. *Angew. Chem., Int. Ed.* **1991**, *30*, 1472–1474. (b) Custelcean, R.; Delmau, L. H.; Moyer, B. A.; Sessler, J. L.; Cho, W.-S.; Gross, D.; Bates, G. W.; Brooks, S. J.; Light, M. E.; Gale, P. A. *Angew. Chem., Int. Ed.* **2005**, *44*, 2537–2542. (c) Mele, A.; Metrangolo, P.; Neukirch, H.; Pilati, T.; Resnati, G. *J. Am. Chem. Soc.* **2005**, *127*, 14972–14973. (d) Cametti, M.; Nissinen, M.; Dalla Cort, A.; Mandolini, L.; Rissanen, K. *J. Am. Chem. Soc.* **2007**, *129*, 3641–3648. (e) Mahoney, J. M.; Beatty, A. M.; Smith, B. D. *J. Am. Chem. Soc.* **2001**, *123*, 5847–5848. (f) Miyaji, H.; Collinson, S. R.; Prokeš, I.; Tucker, J. H. R. *Chem. Commun.* **2003**, 64–65. (g) Mahoney, J. M.; Beatty, A. M.; Smith, B. D. *Inorg. Chem.* **2004**, *43*, 7617–7621. (h) Mahoney, J. M.; Stucker, K. A.; Jiang, H.; Carmichael, I.; Brinkmann, N. R.; Betty, A. M.; Noll, B. C.; Smith, B. D. *J. Am. Chem. Soc.* **2005**, *127*, 2922–2928. (i) Rudkevich, D. M.; Verboom, W.; Reinhoudt, D. N. *J. Org. Chem.* **1994**, *59*, 3683–3686. (j) Lankshear, M. D.; Cowley, A. R.; Beer, P. D. *Chem. Commun.* **2006**, 612–614. (k) Deetz, M. J.; Shang, M.; Smith, B. D. *J. Am. Chem. Soc.* **2000**, *122*, 6201–6207. (l) Shukla, R.; Kida, T.; Smith, B. D. *Org. Lett.* **2000**, *2*, 3099–3102.

Nevertheless, it is worth mentioning that only one example for the detection of an ion pair by fluorescence enhancement has been reported.⁴

Here, we describe the synthesis and binding properties of one ion pair receptor **3** which, acting in a sequential fashion, exhibits remarkable enhancement of the fluorescence in the presence of anions when divalent metal cations are bounded to the cation binding-site. To this end, we have combined in a highly preorganized system the redox activity of the ferrocene group with the fluorogenic behavior of pyrene and the binding ability of the imidazole ring, which is embedded into the framework of the imidazopyrene ring system. The multiresponsive character of the receptor **3** and the ability of the previously unreported imidazopyrene ring system to act not only as a fluorescent antenna but also as favorable binding for cations and anions in the recognition event are most noteworthy.

Receptor **3** was prepared in excellent yield by condensation of pyrene-4,5-dione, available by oxidation of pyrene with the system ruthenium(III) chloride and sodium periodate in CH₃CN at room temperature,⁵ with formylferrocene in the presence of NH₄OAc following an improved modification⁶ of the previously reported method for related compounds⁷ (Scheme 1).

Scheme 1. Preparation of Dyad **3**



The chemosensor behavior of **3** toward a variety of cations (Li⁺, Na⁺, K⁺, Mg²⁺, Ca²⁺, Ni²⁺, Cu²⁺, Zn²⁺, Cd²⁺, Hg²⁺, and Pb²⁺) and anions (F⁻, Cl⁻, Br⁻, AcO⁻, NO₃⁻, HSO₄⁻, H₂PO₄⁻, and HP₂O₇³⁻) was investigated by cyclic (CV) and Osteryoung square-wave (OSWV)⁸ voltammetries as well as through spectrophotometric and ¹H NMR techniques. The titration experiments were further analyzed using the computer program Specfit.⁹

The free receptor exhibited a reversible one-electron redox wave typical of a ferrocene derivative, at the halfwave potential value of $E_{1/2} = 608$ mV, calculated versus the decamethylferrocene (DMFc) redox couple. The results obtained on stepwise addition of the above-mentioned metal

ions show that addition of Zn²⁺, Hg²⁺, and Pb²⁺ metal cations causes significant changes in the redox potential of receptor **3**, with a difference found between the $E_{1/2}$ for receptor–metal system and $E_{1/2}$ for the free receptor ($\Delta E_{1/2}$) ranging from 279 mV for Hg²⁺ to 245 mV for Pb²⁺ (see the Supporting Information). However, addition of Cu²⁺ induces the oxidation of the ferrocene moiety (see the Supporting Information). Titration studies with the addition of the above-mentioned set of anions, as their tetrabutylammonium salts (TBA⁺), to an electrochemical solution of receptor **3** ($c = 10^{-3}$ M) in CH₃CN, containing 0.1 M [*n*-Bu₄N]PF₆ as a supporting electrolyte, have also been carried out. Interestingly, the stepwise addition of H₂PO₄⁻ and AcO⁻ induced the progressive appearance of new oxidation waves cathodically shifted by $\Delta E_{1/2} = -95$ mV and $\Delta E_{1/2} = -212$ mV, respectively which are associated with a recognition process. The addition of Cl⁻, Br⁻, NO₃⁻, and HSO₄⁻ anionic species had no effect on their CV and OSWV, even when present in a large excess, whereas F⁻ and HP₂O₇³⁻ induced deprotonation (see the Supporting Information).

Interestingly, upon addition of the H₂PO₄⁻ anion to the electrochemical solution of the [3·Zn]²⁺ complex ($E_{1/2} = 873$ mV) a cathodically shifted oxidation peak appears at $E_{1/2} = 550$ mV. As this value is intermediate between those found for the cationic [3·Zn]²⁺ and the anionic [3·H₂PO₄]⁻ complexes ($E_{1/2} = 513$ mV), the oxidation wave is ascribed to the [3·Zn(H₂PO₄)₂] complex. However, such addition on the [3·Pb]²⁺ species promotes the appearance of the redox peak ascribed to the free receptor **3** (see Supporting Information). This result clearly shows the ability of the electrochemical DPV technique for detecting the formation of the ion pair [3·Zn(H₂PO₄)₂] complex

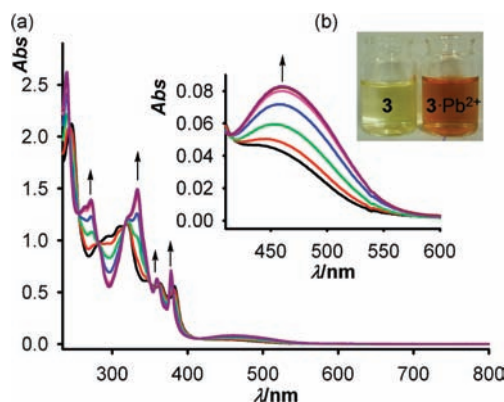


Figure 1. (a) Changes in the absorption spectra of **3** (5×10^{-5} M) in CH₃CN upon addition of increasing amounts of Pb(ClO₄)₂, until 1 equiv (purple). (b) Visual features observed by passing from **3** to the complex **3**·Pb²⁺.

Ion recognition properties of the receptor **3** toward metal cations and anions have also been studied by using absorption and emission techniques. The UV–vis spectrum of receptor **3** in CH₃CN ($c = 5 \times 10^{-5}$ M) exhibits two bands at $\lambda = 364$ nm ($\epsilon = 610$ M⁻¹ cm⁻¹) and 383 nm ($\epsilon = 578$ M⁻¹ cm⁻¹).

(4) de Silva, A. P.; McClean, G. D.; Pagliari, S. *Chem. Commun.* **2003**, 2010–2011.

(5) Hu, J.; Zhang, D.; Harris, F. W. *J. Org. Chem.* **2005**, *70*, 707–708.

(6) Zapata, F.; Caballero, A.; Espinosa, A.; Tárraga, A.; Molina, P. *J. Org. Chem.* **2008**, *73*, 4034–4044.

(7) Steck, E. A.; Day, A. R. *J. Am. Chem. Soc.* **1943**, *65*, 452–456.

(8) OSWV technique has been employed to obtain well-resolved potential information: (a) Serr, B. R.; Andersen, K. A.; Elliot, C. M.; Anderson, O. P. *Inorg. Chem.* **1988**, *27*, 4499–4504. (b) Richardson, D. E.; Taube, H. *Inorg. Chem.* **1981**, *20*, 1278–1285.

(9) Specfit/32 Global Analysis System, 1999–2004; Spectrum Software Associates: Singapore, 1999–2004; <http://www.bio-logic.info/specfits-upt/index.html>.

The addition of Zn^{2+} , Hg^{2+} , and Pb^{2+} cations to a solution of receptor **3** elicited the same optical response. In all cases, the addition of such divalent cations caused the progressive appearance of a new LE band located at $\lambda = 461$ nm, as well as a blue-shift by $\Delta\lambda = 5$ nm of the original two absorption bands. Three well-defined isosbestic points at 375, 380, and 415 nm indicated that neat interconversion between the uncomplexed and complexed species occurs. The new LE band is responsible for the change of color, from yellow to orange which can be used for a “naked eye” detection of these metals (Figure 1). Binding assays using the method of continuous variations (Job’s plot) suggest a 2:1 (receptor/cation) binding model, the global association constants being $\beta = 1.68 \times 10^{10} \text{ M}^{-2}$ for Pb^{2+} , $\beta = 7.28 \times 10^{10} \text{ M}^{-2}$ for Hg^{2+} , and $\beta = 8.71 \times 10^{10} \text{ M}^{-2}$ for Zn^{2+} .

Titration studies of receptor **3** toward the same set of anions revealed that only H_2PO_4^- and AcO^- induced detectable changes. The most prominent feature observed upon addition of successive substoichiometric amounts of these anions is an increase in the intensity of the absorption bands. In these cases, 1:1 binding models were observed and the corresponding binding constants were determined by the analysis of the spectral titration data, $K_a = 8.22 \times 10^5 \text{ M}^{-1}$ for AcO^- and $1.54 \times 10^5 \text{ M}^{-1}$ for H_2PO_4^- .

Assessments of the ion affinities also came from observing the extent to which the fluorescence intensity of receptor **3** was affected in the presence of anions and cations. As expected, receptor **3** showed a weak fluorescence in CH_3CN ($c = 10^{-5} \text{ M}$) revealing that the excitation spectrum at $\lambda_{\text{exc}} = 350$ nm is an ideal excitation wavelength. The emission spectrum displays two well-defined emission bands at 382 and 402 nm, ascribed to the monomeric emission, with a rather low quantum yield ($\Phi = 8 \times 10^{-3}$). Upon addition of Zn^{2+} , Hg^{2+} , and Pb^{2+} cations a remarkable increase of the emission bands at 382 and 402 nm was observed along with a red-shifted structureless maximum at 502 nm probably due to excimer fluorescence (Figure 2).

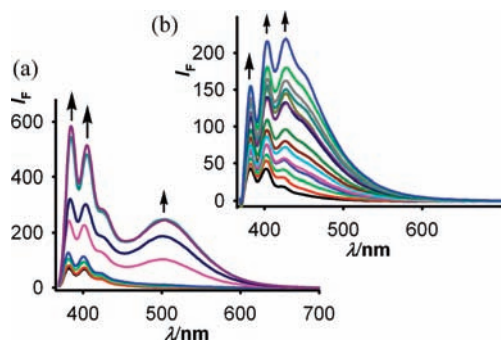


Figure 2. Changes in the fluorescence emission spectra of **3** (black) ($c = 1 \times 10^{-5} \text{ M}$ in CH_3CN) upon addition of increasing amounts of (a) $\text{Pb}(\text{ClO}_4)_2$ until 0.5 equiv (purple) and (b) $[(n\text{-Bu}_4\text{N})\text{H}_2\text{PO}_4]$ until 2 equiv (blue).

The ratio of the fluorescence intensity $\lambda_{402}/\lambda_{502}$ was 1.80 for Zn^{2+} , 1.60 for Hg^{2+} , and 1.83 for Pb^{2+} , and the

quantum yields ($\Phi = 9.2 \times 10^{-2}$ for Zn^{2+} , 8.9×10^{-2} for Hg^{2+} , and 1.02×10^{-1} for Pb^{2+}) resulted in about a 13-fold increase compared to that of receptor **3**.

The stoichiometries of the complexes were determined by the changes in the fluorogenic response of **3** in the presence of varying concentrations of these metal cations, and the obtained result also indicates the formation of 2:1 complexes with global association constants: $\beta = 4.40 \times 10^{10} \text{ M}^{-2}$ for Zn^{2+} , $5.78 \times 10^{10} \text{ M}^{-2}$ for Hg^{2+} , and $7.78 \times 10^{10} \text{ M}^{-2}$ for Pb^{2+} . Interestingly, the addition of 1 equiv of AcO^- and H_2PO_4^- anions also produced an intensity increase of the monomeric emission band at 382 and 402 nm, albeit lower than that originated by the above-mentioned metal cations. An additional strong emission band was also observed at 430 nm (Figure 2b). Fluorogenic titrations indicate the formation of 1:1 complexes giving association constants K_a of $6.62 \times 10^5 \text{ M}^{-1}$ for AcO^- and $1.21 \times 10^5 \text{ M}^{-1}$ for H_2PO_4^- , and the quantum yields ($\Phi = 8.3 \times 10^{-2}$ for AcO^- , 4.6×10^{-2} for H_2PO_4^-) resulted from an 8- to 14-fold increase compared to that of receptor **3**.

Next, titrations with cations were carried out in the presence of anions. The addition of 0.5 equiv of cations to a solution containing the preformed complex $[\mathbf{3} \cdot \text{H}_2\text{PO}_4]^-$ results in the appearance of a red-shifted broad emission band at 422 nm, whose intensity is higher for Pb^{2+} ($\lambda_{422}/\lambda_{402} = 2.02$) and Hg^{2+} ($\lambda_{422}/\lambda_{402} = 1.89$) than for Zn^{2+} ($\lambda_{422}/\lambda_{402} = 0.89$).¹⁰ Identical results were obtained by changing the addition sequence: addition of 2 equiv of anions to a solution of the preformed $[\mathbf{3}_2 \cdot \text{M}]^{2+}$ complex (M: Zn, Hg, Pb). So we believe this emission band at 422 nm is due to the formation of the $[\mathbf{3}_2 \cdot \text{M} \cdot (\text{H}_2\text{PO}_4)_2]$ ion pair complex (Figure 3). When the titrations were carried out on the preformed $[\mathbf{3} \cdot \text{AcO}]^-$ complex, the changes were much lower.

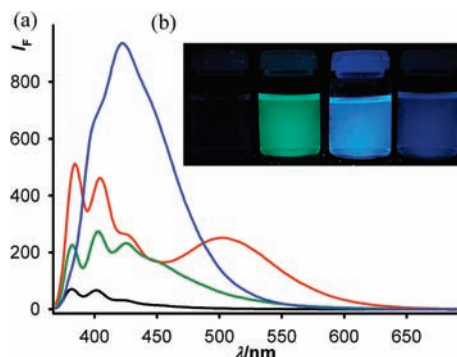


Figure 3. (a) Changes in the fluorescence emission spectra of **3** (black) ($c = 1 \times 10^{-5} \text{ M}$ in CH_3CN) in the presence of 0.5 equiv of $\text{Pb}(\text{ClO}_4)_2$ (red); 2 equiv of $[(n\text{-Bu}_4\text{N})\text{H}_2\text{PO}_4]$ (green); and 0.5 equiv of $\text{Pb}(\text{ClO}_4)_2$ plus 2 equiv of $[(n\text{-Bu}_4\text{N})\text{H}_2\text{PO}_4]$ simultaneously (blue). (b) Visual features observed; from left to right: **3**, **3** + Pb^{2+} , **3** + Pb^{2+} + H_2PO_4^- , **3** + H_2PO_4^- .

To seek more detailed information on the binding properties of receptor **3** with cations and anions, ^1H NMR titration

(10) From the titration data, the β values were found to be of the same order as those found in the titration of the free receptor.

experiments were carried out in DMSO- d_6 . Upon gradual addition of Hg^{2+} cations (0.5 equiv) to a solution of **3** the pyrene protons are downshifted by 0.1–0.2 ppm, whereas the monosubstituted cyclopentadienyl protons are shifted by 0.20–0.30 ppm. Likewise, addition of the H_2PO_4^- anion (1 equiv) induced only an appreciable downshift by 0.15 ppm of the H1 and H8 pyrene protons adjacent to the imidazole ring, whereas the α -ferrocenyl protons are downshifted by 0.21 ppm and the β -protons are upshifted by 0.10 ppm (Figure 4). Shifts of the ferrocene CH protons have already been observed before in some electrochemical sensors for anions.¹¹ Solubility problems do not allow a study with anions and cations simultaneously.

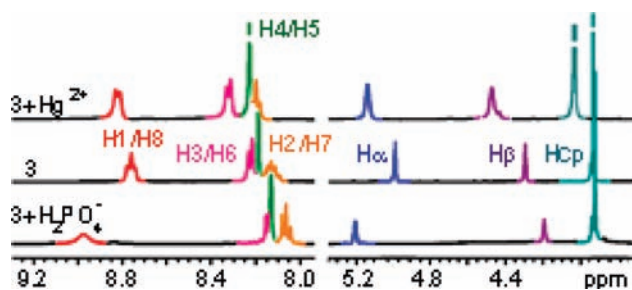


Figure 4. Evolution of ^1H NMR spectra of **3** (middle), in DMSO- d_6 , upon addition of 0.5 equiv of $\text{Hg}(\text{OTf})_2$ (up) and upon addition of 1 equiv of $[(n\text{-Bu}_4\text{N})]\text{H}_2\text{PO}_4$ (down).

Further insight into the binding mode of the reported ion pair complexes was provided by DFT calculations and analyzed utilizing AIM (atoms-in-molecules) methodology.¹² In the case of mercury, the most stable C_2 -symmetric complex shows a well-defined receptor-separated ion pair structure (Figure 5),¹³ sketched as $[(\text{H}_2\text{PO}_4) \cdot \mathbf{3} \cdot \text{Hg} \cdot \mathbf{3} \cdot (\text{H}_2\text{PO}_4)]$, in which binding of every ion cooperatively enhances binding of the others. Thus, the moderately basic H_2PO_4^- anions partially deprotonate the imidazole NH group ($d_{\text{O} \cdots \text{HN}} = 1.340 \text{ \AA}$, $\text{WBI}_{\text{O} \cdots \text{HN}} = 0.245$, $\rho(\mathbf{r}_{\text{C}})_{\text{O} \cdots \text{HN}} = 11.51 \times 10^{-2} \text{ e}/a_0^3$; $d_{\text{N-H}} = 1.174 \text{ \AA}$, $\text{WBI}_{\text{N-H}} = 0.506$, $\rho(\mathbf{r}_{\text{C}})_{\text{N-H}} = 22.27 \times 10^{-2} \text{ e}/a_0^3$) therefore strengthening the ligand–metal bond ($d_{\text{N-Hg}} = 2.092 \text{ \AA}$, $\text{WBI}_{\text{N-Hg}} = 0.449$, $\rho(\mathbf{r}_{\text{C}})_{\text{N-Hg}} = 11.69 \times 10^{-2} \text{ e}/a_0^3$). The essentially linear dicoordination around the

(11) Gale, P. A.; Hursthouse, M. B.; Light, M. E.; Sessler, J. L. *Tetrahedron Lett.* **2001**, *42*, 6759–6762.

(12) Bader, R. F. W. *Atoms in Molecules: A Quantum Theory*; Oxford University Press: Oxford, 1990.

(13) Figure 5 was generated with AMD: Humphrey, W.; Dalke, A.; Schulten, K. *J. Molec. Graphics* **1996**, *14*, 33–38 (<http://www.ks.uiuc.edu/Research/vmd/>).

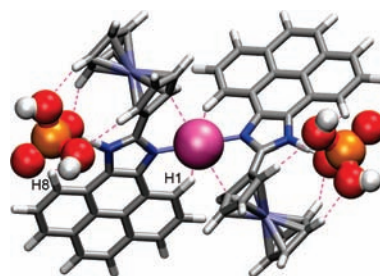


Figure 5. Calculated structure for the $[\mathbf{3}_2 \cdot \text{Hg} \cdot (\text{H}_2\text{PO}_4)_2]$ complex.

Hg^{2+} cation is complemented by two cation- π type interactions with adjacent ferrocenyl C atoms ($d_{\text{C} \cdots \text{Hg}} = 3.046 \text{ \AA}$, $\text{WBI}_{\text{C} \cdots \text{Hg}} = 0.035$, $\rho(\mathbf{r}_{\text{C}})_{\text{C} \cdots \text{Hg}} = 1.71 \times 10^{-2} \text{ e}/a_0^3$) as unambiguously evidenced by the presence of the corresponding bond critical point (BCP) featuring a relatively high ellipticity ($\epsilon = 1.133$). Moreover, the rigid imidazopyrene frameworks locate two H1 ring protons pointing toward the central Hg^{2+} cation ($\text{C-H} \cdots \text{Hg}$ angle 133.0°) allowing the formation of complementary anagostic¹⁴ bonds ($d_{\text{H} \cdots \text{Hg}} = 2.662 \text{ \AA}$, $\text{WBI}_{\text{H} \cdots \text{Hg}} = 0.017$, $\rho(\mathbf{r}_{\text{C}})_{\text{H} \cdots \text{Hg}} = 1.40 \times 10^{-2} \text{ e}/a_0^3$). A set of secondary contacts (with pyrene H8 and ferrocene H atoms) also reinforces the binding to every peripheral H_2PO_4^- anion ($\Sigma\text{WBI} = 0.010$, $\Sigma\rho(\mathbf{r}_{\text{C}}) = 3.08 \times 10^{-2} \text{ e}/a_0^3$).

In conclusion, the ferrocene–imidazopyrene dyad **3** behaves as a host-separated ion pair receptor. A salient feature of this simple receptor is the presence of only one receptor site, the imidazole ring, which is able simultaneously to recognize an anion and a cation through variation of the oxidation potential of the ferrocene/ferrocinium redox couple and a remarkable perturbation of the emission spectrum.

Acknowledgment. We acknowledge the financial support from MICINN-Spain, Project CTQ2008-01402 and Fundación Séneca Project 04509/GERM/06

Supporting Information Available. General experimental comments. Titration spectral data. This material is available free of charge via the Internet at <http://pubs.acs.org>.

(14) Anagostic M–H–C bonds are best described as a “hydrogen bond” involving a 3-center-4-electron orbital interaction with an electrostatic contribution in which the metal serves as a hydrogen bond acceptor. They are characterized by relatively long $\text{M} \cdots \text{H}$ distances ($\sim 2.3\text{--}3.2 \text{ \AA}$) and large M–H–C angles ($\sim 110\text{--}170^\circ$).